Scaling for selectivity in finite nanopores for 1:1 electrolytes: the dependence of predictability of device behavior on system parameters

Zsófia Sarkadi, Zoltán Ható, Mónika Valiskó, Dezső Boda*

Center for Natural Sciences, University of Pannonia, Egyetem u. 10, Veszprém, 8200, Hungary

Abstract

The scaling properties of a cation selective nanopore mean that the device function (selectivity) depends on the input parameters (pore radius, pore length, surface charge density, electrolyte concentration, voltage) via a single scaling parameter that is a simple analytical function of the input parameters. In our previous study (Sarkadi et al., J. Mol. Liq., 357 (2022) 119072.), we showed that a parameter inspired by the Dukhin number (therefore, we also call it a Dukhin number) is an appropriate scaling parameter for infinitely long nanopores. Here, we extend that study to finite pores in a membrane and provide a detailed analyzes over a large parameter space for 1:1 electrolytes obtained from the Nernst-Planck transport equation coupled either to the Local Equilibrium Monte Carlo method or to the Poisson-Botzmann theory. Scaling is exact in a limiting case, where an analytical solution, such as Linearized Poisson-Boltzmann, is available (infinite pore). Here we show that scaling can work even if the solution is numerical or provided by computer simulations (finite pore). We discuss how these cases approach the limiting case as functions of the system parameters.

1. Introduction

Nanopores facilitate the controlled transport of ions between two bath electrolytes through an insulating membrane. The nature of control depends on the properties of the nanopore. These properties include the geometry of the pore (length, radius), external conditions, and the chemical groups anchored on its wall. External conditions include the properties and concentrations of the electrolytes in the embedding baths and the voltage applied across the membrane. The chemical groups determine the surface charge pattern on the nanopore's wall, and the applicability of the device as a sensor or a DNA sequencer, for example.

A particular case that is our interest is when a uniform surface charge density is placed on the wall of the nanopore making the pore selective for cations or anions depending on the sign of the surface charge. In this case, an electrical double layer (DL) is formed near the wall where surface conductance dominates. If the width of the DL is smaller than the radius of the pore, a bulk solution is formed near the centerline of the nanopore where volume conductance dominates (Fig. 1).

If we consider the nanopore and the surrounding baths as a device, we can define *input parameters* (length, H, radius, R, surface charge density, σ, concentration, c, ionic valences, $z_+ : z_-$, and voltage, U) and *output parameters* (electrical current, I_i, or particle current, J_i, carried by ionic species i; their relation is $I_i = z_i e J_i$ where e is the unit charge). The relationship between the input and output quantities is called the *device function*.

The question that we posed in a series of studies [1–6] is whether we can predict the behavior of the nanopore for different combinations of the input parameters on the basis of a simple principle that we call scaling. By scaling we mean that the output parameters depend on the input parameters via a single scaling parameter, ξ, that is a simple analytical function of the input parameters, $\xi(a_1, a_2, \dots)$, and that the device function, F, is a smooth unambiguous function of the scaling parameter: $F = f[\xi(a_1, a_2, \dots)]$.

Any monotonic function of the currents (I_i or J_i) is also a device function. In this study, the device function is cation selectivity ($\sigma \leq 0$) defined as

$$S_+ = \frac{|J_+| - |J_-|}{|J_+| + |J_-|}. \tag{1}$$

If we assume that $|J_+| = |J_-|$ for a non-selective pore (with the assumption that the diffusion co-

*Author to whom correspondence should be addressed.
E-mail address: boda@almos.vein.hu

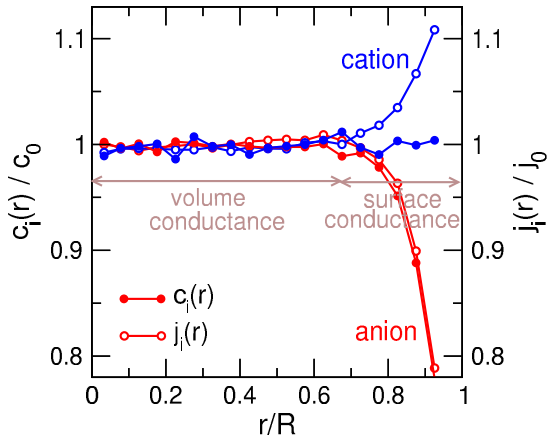

Figure 1: Illustration of regions of volume conductance (where the $c_i(r)$ and $j_i(r)$ profiles are constant and bulk-like) and surface conductance (where the $c_i(r)$ and $j_i(r)$ profiles for cations (blue) and anions (red) separate). The concentration profiles, $c_i(r)$, and the z-component of the flux profiles, $j_i(r)$, have been normalized by the bulk values at $r \approx 0$ denoted by c_0 and j_0, respectively. The figure shows NP+LEMC results for $R = 4$ nm, $H = 6$ nm, $\sigma = -0.1$ e/nm^2, and $U = 10$ mV. The profiles obtained in the middle of the pore, $z \approx 0$, are shown.

efficients are the same, $D_+ = D_-$), this function varies between 0 and 1 from the perfectly non-selective case ($\sigma = 0$) to the perfectly selective case ($\sigma \to -\infty$). The real situation is somewhere between these extremes.

In a previous work [5] we showed that in the infinitely long pore ($H \to \infty$) and the slope conductance ($U \to 0$) limit, the scaling parameter is

$$\text{Du} = \frac{(z_+ + |z_-|)\,\text{Du}^0}{2 + (z_+ - |z_-|)\,\text{Du}^0}, \tag{2}$$

where

$$\text{Du}^0 = -\frac{\sigma 8\pi l_\text{B} \lambda_\text{D}^2}{eR}. \tag{3}$$

Here

$$\lambda_\text{D} = \left(\frac{ce^2}{\epsilon_0 \epsilon kT} \sum_i z_i^2 \nu_i \right)^{-1/2}, \tag{4}$$

is the Debye length, ϵ is the dielectric constant of the solvent (78.45 in this work), ϵ_0 is the permittivity of vacuum, $l_\text{B} = e^2/4\pi\epsilon_0\epsilon kT$ is the Bjerrum length, k is Boltzmann's constant, T is temperature (298.15 K in this work), and ν_i is the stoichiometric coefficient of ionic dissociation. Eq. 2 is valid for any z_+ and z_-. For a 1:1 electrolyte (considered in this work), $\text{Du} = \text{Du}^0$. Note that the system's behavior is different for different signs of σ if the electrolyte is asymmetric.

A related parameter was introduced earlier in several studies [7–20] in the form

$$\text{Du}^\text{Bikerman} = \frac{|\sigma|}{eRc}, \tag{5}$$

which is a dimensionless number if we take concentration in the appropriate unit. It is equivalent with Eq. 3 for 1:1 electrolytes. It was called the Bikerman-Dukhin number [7, 8] or just Dukhin number. [9–20] The name was introduced by Lyklema to salute Dukhin [21], hence the notation Du.

The Dukhin number was originally used to characterize the ratio of the surface and volume conductances [22–27] that are output properties of the measurement or calculation. On the contrary, the Dukhin number in Eq. 5 contains input parameters. Relating these two ways of defining the Dukhin number practically carries the core idea of scaling.

Scaling holds if an analytical theory provides the necessary relation between the input and output parameters. The Linearized Poisson-Boltzmann (LPB) theory is an analytical theory that provides the simple analytical relation $S_+ = \text{Du}$ between the scaling parameter, Du, and the device function, S_+, in the $H \to \infty$, $U/H \to 0$, and $\text{Du} \to 0$ limits. [5]

At larger values of Du, the full PB is solved numerically, so the relation is not analytical anymore, but still unambiguous for a fixed value of λ_D/R. For different values of λ_D/R, different curves are obtained for large Du values as shown in Fig. 2A. The inset shows the $S_+ = \text{Du}$ equality for small values of Du, while the full curves show that the agreement between the $c = 0.01$ and 0.1 M results is good, while deviation occurs for $c = 1$ M, where LPB does not work so well.

Fig. 2A shows S_+ as a function of $\text{Du} = \text{Du}^0$ on a logarithmic scale for the Du-axis. The obtained curve is a sigmoid with the lower branch corresponding to less selective pores, while the upper branch corresponding to more selective pores. The inflection point can be regarded as a point that separates these two regimes. In this work, by inflection point we mean the Du^infl value at which the selectivity is 0.5, namely

$$S_+(\text{Du}^\text{infl}) = 0.5. \tag{6}$$

We say that scaling works if the sigmoid curves collapse onto one single curve ("master curve") for different parameters of the system. The collapse works if the inflection points are the same. Scaling, therefore, can be characterized by the inflection point, Du^infl.

Equation 2 provides a new scaling parameter, Du, for asymmetric electrolytes that is a rational function of Du^0 with a domain of $[0 : (z_+ + |z_-|)\text{Du}^0/2]$ that is [0 : 1.5] for 2:1 electrolytes and [0 : 2] for 3:1 electrolytes. Using that rational function, we have a parameter of finite domain, so we

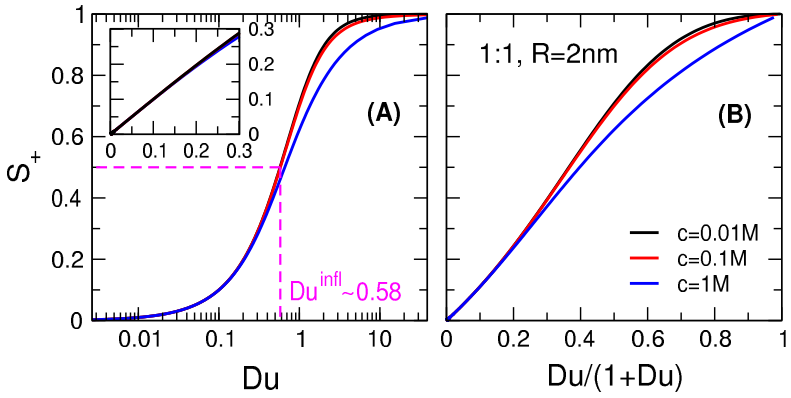

Figure 2: Selectivity curves for an infinite nanopore ($H \to \infty$) obtained by scanning the surface charge ($-3 \le \sigma \le -0.001$ e/nm^2) as functions of the Dukhin number (Eq. 2) for 1:1 electrolytes for $R = 2$ nm at different concentrations, namely, varying the λ_D/R values. The curves have been obtained by numerically solving the nonlinear PB equation in equilibrium ($U = 0$ V). Panel A shows S_+ as a function of Du using a logarithmic scale for Du. The resulting selectivity curves are sigmoids. The inset shows the same data for small Du values but using a linear scale. In this regime, the LPB theory provides the analytical solution, $S_+ = \mathrm{Du}$. Panel B shows the same data as a function of Du/(1+Du). The data are from Ref. [5].

can plot the scaling curve on a linear scale of the Du-axis.

Inspired by this, we introduce a new scaling parameter for 1:1 electrolytes as

$$\frac{\mathrm{Du}}{1+\mathrm{Du}} \tag{7}$$

that has the domain $[0:1]$ and the slope 1 as $\mathrm{Du} \to 0$. The curves of Fig. 2A are plotted again in Fig. 2B as functions of Du/(1+Du). The messages of panels A and B are the same, but panel B shows the results in a more concise way in a 1×1 square. Therefore, we show scaling curves using this parameter in this paper, and when it comes to a single number to characterize scaling, we use the inflection point, Du$^{\mathrm{infl}}$.

The PB results shown in Fig. 2 agree relatively well with Grand Canonical Monte Carlo (GCMC) simulation results for the inifinite nanopore. [5] This indicates that 1:1 electrolytes at room temperature and $\epsilon = 78.45$ can be handled with the mean-field PB theory. It is a general finding that scaling works better if analytical, or, at least, mean-field theories are applicable. This is not the case for multivalent electrolytes where ionic correlations are strong. [2, 3, 5]

Scaling is also problematic if the nanopore is short compared to its radius, namely, when the aspect ratio H/R is small. In our previous paper [4] we studied nanopores of finite lengths. We considered nanopores from the nanotube limit ($H/R \to \infty$) to the nanohole limit ($H/R \to 0$) for 1:1 systems, and showed that Du is not applicable anymore as the length of the pore decreases. We showed for 1:1 electrolytes in the nanohole limit that using a rescaled version of Du called the modified Dukhin number is advantageous:

$$\mathrm{mDu} = \mathrm{Du}\frac{H}{\lambda_D} = -\frac{\sigma 8\pi l_B \lambda_D H}{eR} \tag{8}$$

mDu seemed appropriate for short nanopores; what is more, it proved to be the right scaling parameter for bipolar nanopores where the device function is rectification. [6]

In this work, we change the parameters, H, R, σ, c, and U ($z_+ = 1$ and $z_- = -1$ are fixed), and see how the selectivity curves behave. This is a large and complex space of variables, so it required a large number of simulations, much more than published in Ref. [4]. To make our point, we need to present our results in a well-organized systematic way: by fixing all parameters and (1) changing only one, or (2) changing the ratio of two (λ_D/R, λ_D/H, and H/R).

2. Model and method

A cylindrical nanopore of length H and radius R spans a membrane that separates two baths. The thickness of the membrane is H. The cylindrical wall of the nanopore and the flat parallel walls confining the membrane are assumed to be hard. This means that the ions modeled as charged hard spheres (Eq. A.1) cannot overlap with these walls.

Ion transport (drift-diffusion) is computed with the Nernst-Planck (NP) equation (Eq. A.2) that contains the concentration profile, $c_i(\mathbf{r})$, and the gradient of the chemical potential profile, $\nabla\mu_i(\mathbf{r})$ as the driving force. The relation between $c_i(\mathbf{r})$

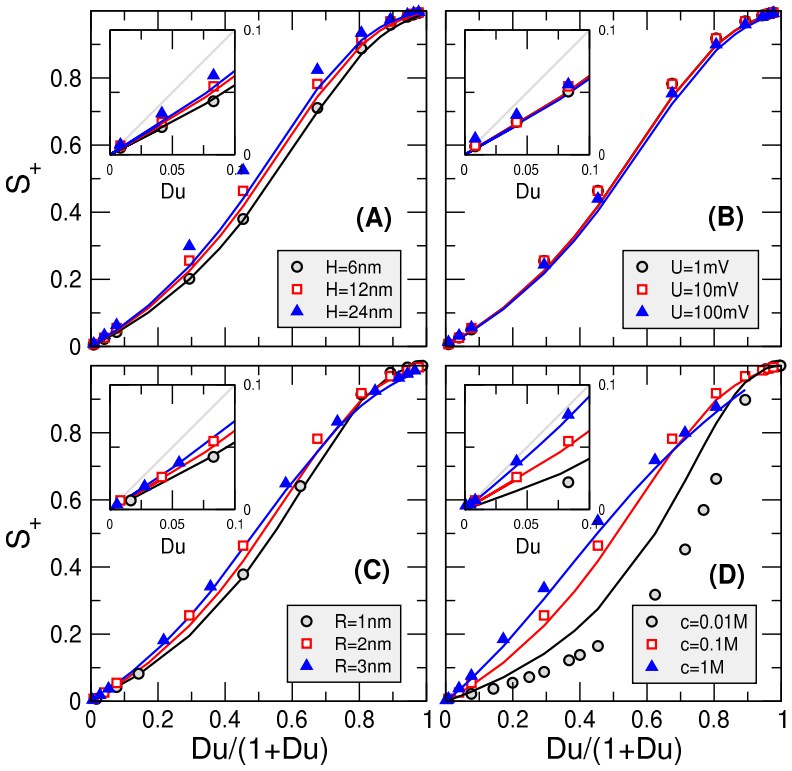

Figure 3: Selectivity curves obtained by scanning the surface charge ($-3 \le \sigma \le -0.001$ e/nm^2) as functions of Du/(1+Du). A base point, $H = 12$ nm, $R = 2$ nm, $U = 10$ mV, and $c = 0.1$ M, has been specified (red color), and one parameter is systematically changed in each panel while the others are kept fixed (H, U, R, and c are changed in panels A, B, C, and D, respectively) The insets show the data as a function of Du for small Du values (small σ). The gray lines show the theoretical limiting case with slope 1, where $S_+ = \mathrm{Du}$ that has been obtained from the LPB theory for the infinite nanopore limit [5]. Symbols and lines show NP+LEMC and PNP results, respectively.

and $\mu_i(\mathbf{r})$ is provided either by the PB theory, or a non-equilibrium variant of GCMC simulation, the Local Equilibrium Monte Carlo (LEMC) method. [28] When PB is coupled to the NP equation, we obtain the Poisson-Nernst-Planck (PNP) theory. [29, 30] When LEMC is coupled to the NP equation, we obtain the NP+LEMC method. [31]

In both cases, the system is solved numerically by dividing the domain of solution into small volume elements. An iterative procedure provides a self-consistent solution also satisfying the continuity equation, $\nabla \cdot \mathbf{j}_i(\mathbf{r}) = 0$.

A basic difference between PNP and NP+LEMC is that the latter contains all the many-body correlations (electrostatic and hard sphere) beyond the mean-field approximation of PNP. In PNP, the excess chemical potential of an ionic species is the interaction of the ion with the mean electrical potential produced by all the ions and charges in the system including the external electric field.

More details are found in Appendix A.

3. Results and Discussion

In the following, we uncover the behavior of the system in the parameter space $\{\sigma, H, R, c, U\}$. First, we show cases when scaling works; then, we focus on cases when scaling fails, and we discuss the reasons.

3.1. The base point and dependence on individual parameters

Let us define a base point, where scaling works quite well: $H = 12$ nm, $R = 2$ nm, $U = 10$ mV, and $c = 0.1$ M. The surface charge density, σ, is scanned from zero to high (negative) values (sometimes even beyond physically meaningful values) to produce the selectivity curves seen in Fig. 3. This means that we cover the (0 : 1) range in Du/(1 + Du).

Fig. 3 shows that the slopes are smaller than 1 (see insets), because the nanopore is short ($H = 6 - 24$ nm). The slope is closer to 1 for $c = 1$ M (panel D), because in this case λ_D is smaller, thus the pore is less selective for a given σ. Accordingly, the shape of the curves is different from those for the infinite pore (compare to Fig. 2). A

given selectivity, S_+, can be achieved only with a larger value of Du, namely, with a larger value of $|\sigma|$. Short pores are less selective than long pores.

The agreement between the NP+LEMC and the PNP data is quite good because electrostatic correlations are relatively weak for a 1:1 elecrolyte at $T = 298.15$ K and $\epsilon = 78.45$. The exception is the $c = 0.01$ M case, where λ_D is so large that the DLs seriously overlap both radially and axially. This case highlights that there are differences between LEMC and PNP regarding electrostatic boundary conditions [30] and approximations in the model.

If we change parameters individually while the others are kept constant, we find that scaling is weakly dependent on the parameters H, U, and R (panels A-C). Concentration, on the other hand, has a large effect (panel D). The explanation is that H, U, and R influence either the radial behavior (R), or the axial behavior (H and U), while c influences both.

3.2. Radial and axial effects

As we already discussed in our previous work [4], we can distinguish radial and axial effects in the finite nanopore system. The ability of the electrolyte to screen the Coulomb forces and, thus, to suppress either radial or axial effects, is characterized by the Debye-length, λ_D. In an infinitely long nanopore only radial effects are present.

Nanopores can influence the conductance properties of the electrolyte because their radius, R, is comparable with the width (λ_D) of the DL that is formed radially at the charged wall of the pore. The ion selective region of the interior of the nanopore is this radial DL (see the surface conductance region in Fig. 1). From the point of view of the overall selectivity of the nanopore, therefore, the counterion content and the width of this region matter (the anions are the counterions in this work). The counterion content is determined by σ, while the width of the DL with respect to R is determined by the λ_D/R ratio (radial concentration profiles are shown in Fig. S1 of the Supplementary Information (SI)).

If λ_D/R is small, the counterions are restricted to a thin layer near the wall, a bulk electrolyte is formed in the centerline of the pore (see Fig. 1), volume conductance dominates, and the nanopore is less selective. If λ_D/R is large, the DLs overlap in the centerline, coions are exluded from the pore, surface conductance dominates, and the nanopore is more selective. Variables λ_D/R and σ together, therefore, has a major effect on the radial behavior of the pore. For long enough nanopores (such as in experiments for PET nanopores), the radial effects in the middle of the pore along the z-axis dominate selectivity, because this central region is far from the entrances of the pore and the axial electric field, $E \sim U/H$, is small.

If the nanopore is short, however, the concentration profiles and selectivity are seriously affected by charge accumulation near the membrane surfaces at the entrances of the pore on the two sides. These axial DLs are formed either because the structural charges of the nanopore are partially neutralized from outside by the counterions accumulated in these DLs or because the polarizing effect of the external electric field (for details see Figs. S2 and S3 of the SI).

The effect of the axial DLs in the middle of the pore can be decreased either by increasing H (Fig. S2 of the SI) or by decreasing U (Fig. S3 of the SI). As λ_D/R in the case of the radial behavior, the relevant parameter is the λ_D/H ratio because it characterizes how far the axial DLs can extend into the pore from the entrances.

The electrolyte concentration has importance in both dimensions, because the ability of the electrolyte to screen electrostatic interactions is relevant, whether we talk about the ability to screen the pore charge in the radial dimension or the ability to screen the membrane charges in the axial dimension.

3.3. Dependence on the R/λ_D ratio

Let us examine the R/λ_D dependence of scaling by plotting the inflection point (Eq. 6) for different values of H in Fig. 4. A given color refers to a given R, while the data points are obtained by changing the concentration: c increases from left to right.

Using R/λ_D as a variable is advantageous because the asymptotic behavior of the curves is better seen: they converge to some limiting values as $R/\lambda_D \to \infty$. These limiting values depend on H: they decrease with increasing H. The nanotube limiting value is

$$\lim_{\substack{H/\lambda_D \to \infty, \\ \lambda_D/R \to 0}} \mathrm{Du}^{\mathrm{infl}} \approx 0.58 \tag{9}$$

indicated by a magenta dashed line in the figure, as also depicted in Fig. 2. The curves approach the limiting value faster if R is smaller, namely, if the aspect ratio, H/R, is larger.

The PNP and NP+LEMC results show the same trend; quantitative deviations can be observed for $R = 1$ and 2 nm due the finite size of the ions.

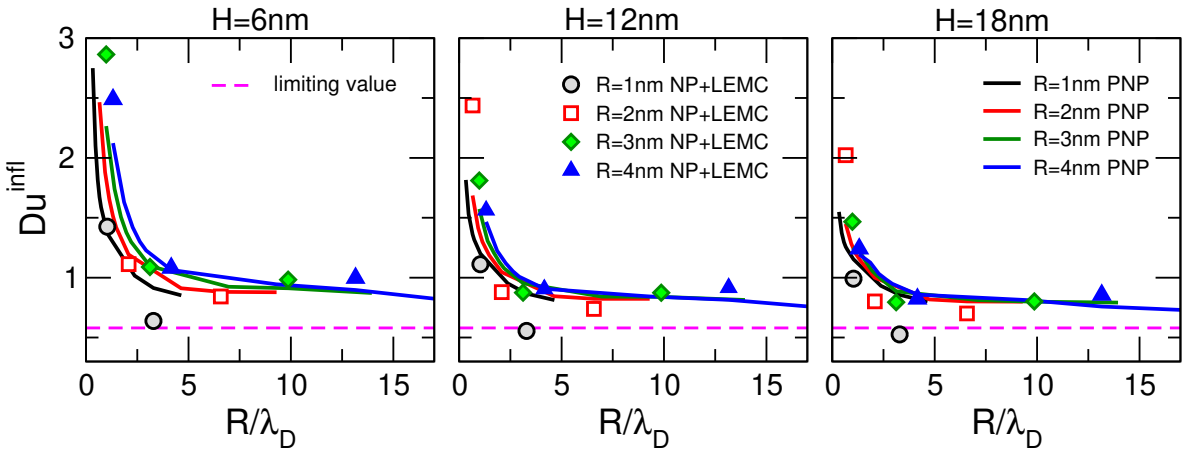

Figure 4: Inflection points, $\mathrm{Du}^{\mathrm{infl}}$ (Eq. 6), as functions of the R/λ_{D} ratio. Various panels refer to various values of H (6, 12, and 18 nm), while various colors refer to various values of R (1, 2, 3, and 4 nm). The data points for a given curve correspond to concentrations $c = 0.01$, 0.1, and 1 M (from left to right). Voltage is $U = 10$ mV. Symbols and lines refer to NP+LEMC and PNP results, respectively. The dashed magenta line indicates the limiting value $\mathrm{Du}^{\mathrm{infl}} \approx 0.58$ in the $H \to 0$, $U \to 0$, $\mathrm{Du} \to 0$ limit.

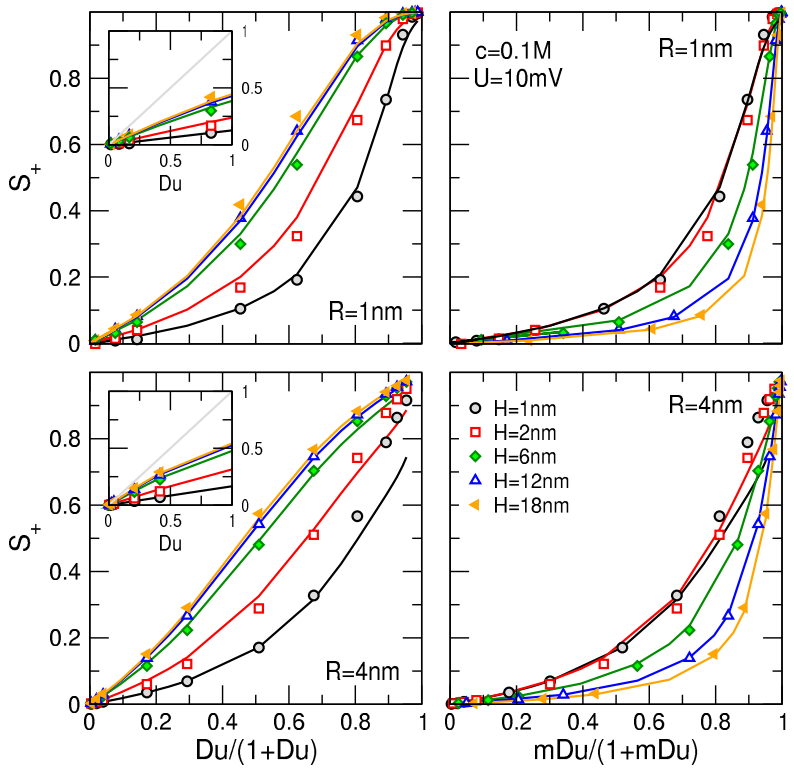

Figure 5: Selectivity curves obtained by scanning the surface charge ($-3 \le \sigma \le -0.001$ e/nm^2) as functions of $\mathrm{Du}/(1+\mathrm{Du})$ (left panels) and $\mathrm{mDu}/(1+\mathrm{mDu})$ (right panels). $\mathrm{mDu} = \mathrm{mDu}^0$ (Eq. 8) for 1:1 electrolytes. Top and bottom panels refer to $R = 1$ and 4 nm, respectively. Various colors refer to various values of H ($H = 1$, 2, 6, 12, and 18 nm). Concentration is $c = 0.1$ M, while voltage is $U = 10$ mV. Symbols and lines refer to NP+LEMC and PNP results, respectively. The insets show the data as functions of Du for small Du values (small σ). The gray lines show the theoretical limiting case with slope 1, where $S_+ = \mathrm{Du}$ that has been obtained from the LPB theory for the infinite nanopore limit [5].

3.4. Dependence on the H/λ_{D} ratio

Let us examine the H/λ_{D} dependence of scaling via the appropriate scaling curves (Fig. 5) and the inflection points (Fig. 6) for different values of R.

Fig. 5 shows S_+ as a function of $\mathrm{Du}/(1+\mathrm{Du})$ (left panels) and $\mathrm{mDu}/(1+\mathrm{mDu})$ (right panels) for varying values of H (indicated by different colors). Top and bottom rows refer to $R = 1$ and 4

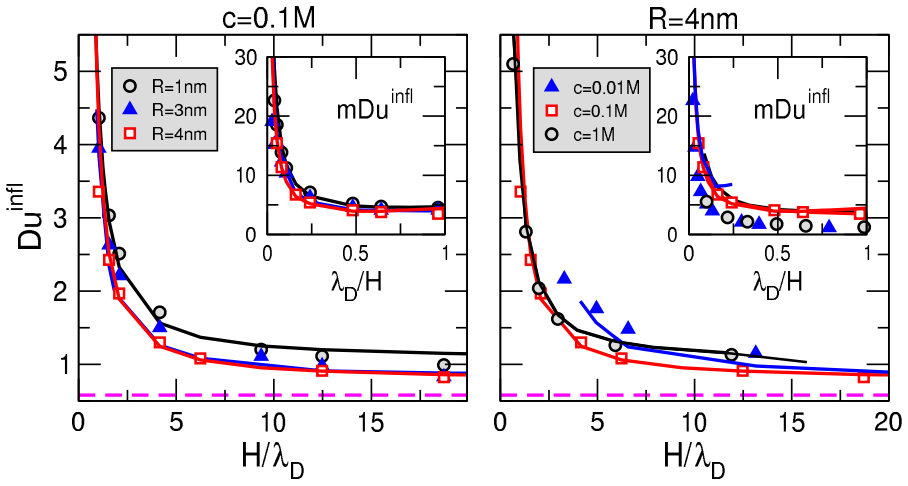

Figure 6: Inflection points of Du (Eq. 6), as functions of the H/λ_D ratio. The insets show the inflection points of mDu (defined similarly to Eq. 6), as functions of the λ_D/H ratio. $\mathrm{mDu} = \mathrm{mDu}^0$ (Eq. 8) for 1:1 electrolytes. The left panel shows results for various pore radii ($R = 1$, 3, and 4 nm) at $c = 0.1$ M, while the right panel shows results for various concentrations ($c = 0.1$, 0.1, and 1 M) at $R = 4$ nm. The curves have been obtained by scanning H from 0.5 to 36 nm. Voltage is $U = 10$ mV. Symbols and lines refer to NP+LEMC and PNP results, respectively. The dashed magenta line indicates the limiting value $\mathrm{Du}^{\mathrm{infl}} \approx 0.58$ in the $H \to 0$, $U \to 0$, $\mathrm{Du} \to 0$ limit.

nm, respectively. The curves have been computed with NP+LEMC (symbols) and PNP (lines) for a wide range of H from 1 nm to 18 nm. The mDu parameter (Eq. 8) was introduced in our previous work [4] and it was shown that it is a more appropriate scaling parameter for short nanopores in the nanohole limit ($H/R \to 0$).

Our present results are in agreement with the findings of Ref. [4] for $c = 0.1$ M. The left panels of Fig. 5 show that the $H = 12$ nm curves collapse onto the $H = 18$ nm curves if we use Du as the scaling parameter. Accordingly, the main panels of Fig. 6 show that the inflection point of Du converges to the nanotube limiting value 0.58 (magenta dashed line; Eq. 9) as $H/\lambda_D \to \infty$. The left panel of Fig. 6 shows R-dependence for $c = 0.1$ M, while the right panel shows c-dependence for $R = 4$ nm.

If we use mDu as the scaling parameter (right panels of Fig. 5), the $H = 1$ nm curves collapse onto the $H = 2$ nm curves. The limiting case now is the nanohole ($H \to 0$) limit that does not produce a single value such as ≈ 0.58 in the nanotube ($H \to \infty$) limit. Here, this limiting value depends on R and λ_D. Furthermore, H cannot be smaller than a physically meaningful minimum value (about the thickness of a graphene sheet). In any case, the inflection points of mDu indicate convergence to some state-dependent value as functions of λ_D/H (insets of Fig. 6) confirming the findings of Ref. [4].

3.5. Dependence on the H/R ratio

Let us examine the H/R (aspect) ratio dependence of scaling by plotting the inflection point (Eq. 6) for different values of c and R in Fig. 7. The curves converge to the nanotube limiting value 0.58 (magenta dashed line) as soon as λ_D/R is small (λ_D is small or R is large).

3.6. Voltage dependence

Voltage dependence was already shown in our previous work [4], but there we showed only PNP data for $R = 1$ nm. Figure 8 shows results for $R = 3$ nm for both the PNP and NP+LEMC methods. Stronger U-dependence can be observed for smaller concentrations ($c = 0.01$ M results are seen in Fig. 9 of Ref. [4]) and for shorter pores.

Voltage dependence is not linear as opposed to our study for bipolar nanopores [6], where mDu rescaled with U linearly ($\mathrm{mDu}\, U/U_0$) proved to be an appropriate scaling parameter.

3.7. Inflection point vs. slope

As it was shown in Ref. [5] for the infinite nanopore ($H/R \to \infty$), the slope of the S_+ vs. Du curve at the $\mathrm{Du} \to 0$ limit is 1 because $S_+ = \mathrm{Du}$ in this limit. The inset of Fig. 2A shows this limiting case for the infinite nanopore and it is also indicated by gray lines in the insets of Figs. 3 and 5.

So far, we used the inflection point as a single parameter to characterize scaling (Figs. 4, 6, 7, and 8). The slope of the S_+ vs. Du curve at the $\mathrm{Du} \to 0$ limit, however, could also be used for this

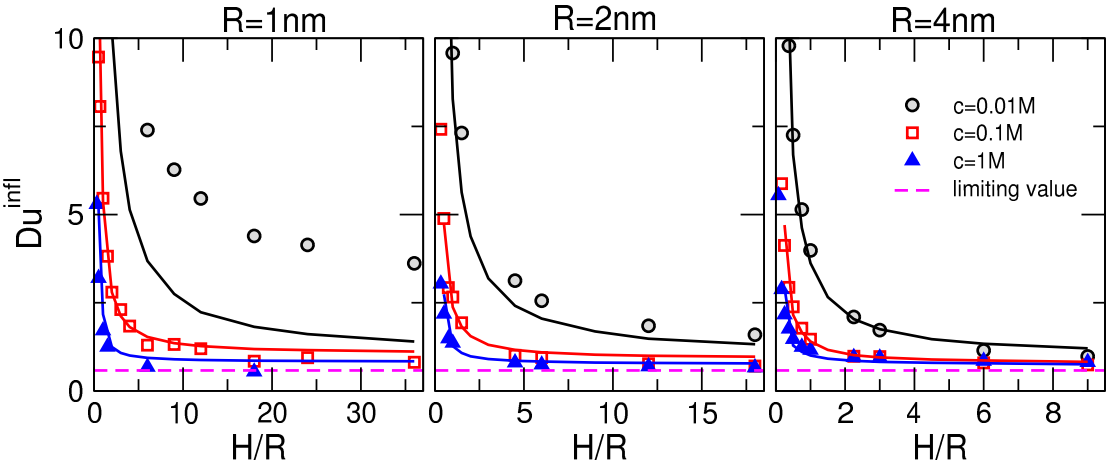

Figure 7: Inflection points of Du (Eq. 6), as a function of the H/R ratio. Various panels refer to various pore radii ($R=1$, 2, and 4 nm from left to right). Various colors refer to various concentrations ($c=0.01$, 0.1, and 1 M). Voltage is $U=10$ mV. Symbols and lines refer to NP+LEMC and PNP results, respectively. The curves have been obtained by scanning H from 1 to 18 nm. The dashed magenta line indicates the limiting value $\mathrm{Du}^{\mathrm{infl}} \approx 0.58$ in the $H \to 0$, $U \to 0$, $\mathrm{Du} \to 0$ limit.

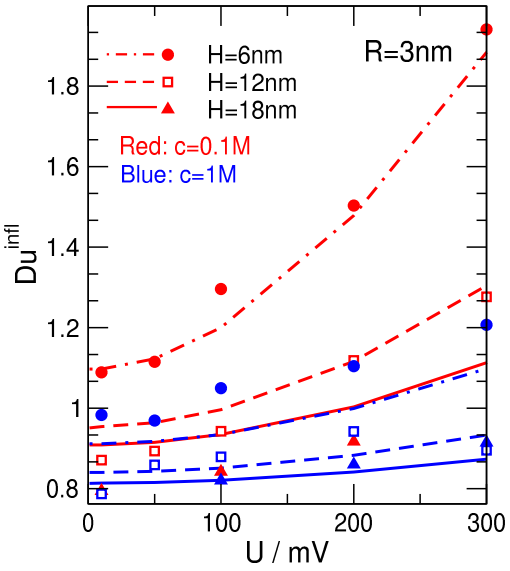

Figure 8: Inflection points of Du (Eq. 6), as a function of voltage, U, for $R=3$ nm. Various curves refer to various values of H ($H=6$, 12, and 18 nm), while colors red and blue refer to concentrations $c=0.1$ and 1 M, respectively. Symbols and lines refer to NP+LEMC and PNP results, respectively.

purpose. In Fig. 9, we collected our results by plotting the inflection points against the slopes. The two panels correspond to $R=1$ and 3 nm, colors correspond to different concentrations, while H increases from left to right for a given c. The limiting values for $\mathrm{Du}^{\mathrm{infl}}$ and the slope, ≈ 0.58 and 1, respectively, are also indicated with magenta dashed lines.

From the behavior of the scaling curves described either as a S_+ vs. $\lg \mathrm{Du}$ function or as a S_+ vs. $\mathrm{Du}/(1+\mathrm{Du})$ function, it is evident that the smaller the slope is, the larger $\mathrm{Du}^{\mathrm{infl}}$ is. This is clearly shown in Fig. 9. The nanotube limiting case corresponds to a single point in the figure given by ≈ 0.58 inflection point and 1 slope. The data points approach this limiting point as c and/or H increases. This convergence is more obvious in the right hand side panel ($R=3$ nm), where hard-sphere effects have less relevance in the case of NP+LEMC.

4. Summary

This study synthesizes the findings of our two previous papers [4, 5] by providing a broader picture on the basis of a more expanded data base obtained with NP+LEMC and PNP calculations. In Ref. [4] we proposed the Dukhin number (Du) to be a useful scaling parameter for finite nanopores and 1:1 electrolytes on the basis of empirical results.

Later in Ref. [5], Du was derived from the PB theory in the nanotube limit ($H \to \infty$, $U \to 0$). The derivation was based on the limiting case of $\mathrm{Du} \to 0$, where LPB provides the analytical solution of $S_+ = \mathrm{Du}$, where Du is a rational function of Du^0 (see Eqs. 2 and 3) . For 1:1 electrolytes, $\mathrm{Du} = \mathrm{Du}^0$.

The idea of scaling is based on analytical solutions and the corresponding limiting cases where these solutions are valid. The question is whether scaling can be extended to cases where analytical solutions are no longer available. Even if scaling is not exact, it can be accurate enough to provide good predictions for device behavior.

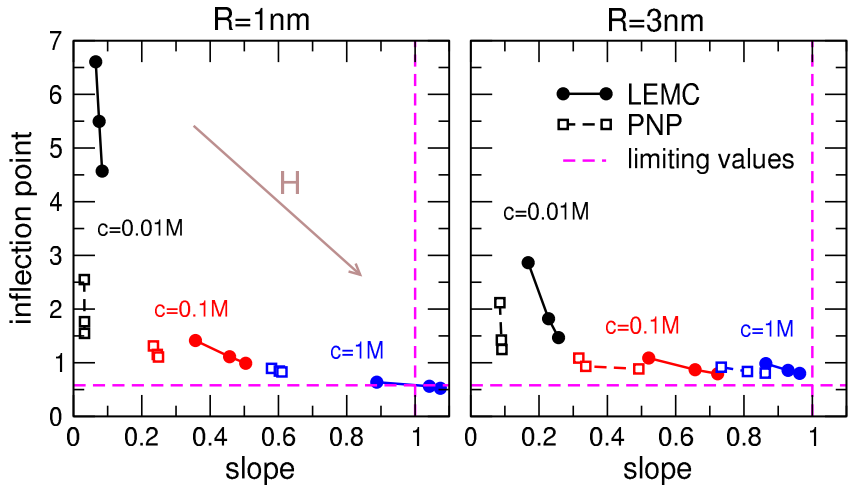

Figure 9: Inflection points of Du (Eq. 6) plotted against the slope of the S_+ vs. Du curves (see the insets of Figs. 2, 3, and 5) for radii $R = 1$ and 3 nm (left and right panels). Colors correspond to various concentrations ($c = 0.01$, 0.1, and 1 M). For a given color, data points correspond to pore lengths $H = 6$, 12, and 18 nm. Voltage is $U = 10$ mV. Filled and open symbols refer to NP+LEMC and PNP results, respectively. The dashed magenta lines indicate the limiting values ($\mathrm{Du}^{\mathrm{infl}} \approx 0.58$ and slope 1) in the $H \to 0$, $U \to 0$, $\mathrm{Du} \to 0$ limit.

For example, scaling is exact for the $\mathrm{Du} \to 0$, $H \to \infty$, $U \to 0$ limits using the LPB theory. For larger values of Du, the numerical solution of the PB theory provides approximate, but still good scaling behavior in the $\lambda_D/R \to 0$ limit. Computer simulations (GCMC) based on the charged hard sphere model of the electrolyte provide good agreement with the mean-field PB calculations as soon the electrostatic correlations are not too strong; practically, for 1:1 electrolytes.

To step forward and to expand the parameter space, two questions should be addressed. (1) What happens if the pore is finite? (2) What happens if the electrolyte is multivalent?

In this work, we consider the first question and study finite pores for 1:1 electrolytes. It was shown already in Ref. [4] that Du is not necessarily an appropriate scaling parameter for pores of finite length. What is more, a rescaled parameter (mDu) appeared to be a better scaling parameter in the nanohole limit ($H \to 0$). Here, we focus our analysis by using the limiting case as a cornerstone and show that the system approaches the limiting case ($\mathrm{Du}^{\mathrm{infl}} \approx 0.58$) as various input parameters are varied, namely, as $\lambda_D/R \to 0$, $\lambda_D/H \to 0$, $R/H \to 0$, and/or $U \to 0$.

The second question will be addressed in a subsequent study, where we discuss whether Du (Eq. 2) is an appropriate scaling parameter for finite nanopores and multivalent electrolytes. This case is complicated by the fact that PNP and NP+LEMC give different results due to the strong electrostatic correlations present in the system.

Acknowledgements

We gratefully acknowledge the financial support of the National Research, Development and Innovation Office – NKFIH K137720 and the TKP2021-NKTA-21. Supported by the ÚNKP-22-3 New National Excellence Program of the Ministry for Culture and Innovation from the source of the National Research, Development and Innovation Fund. We are grateful to Dirk Gillespie and Tamás Kristóf for inspiring discussions.

Appendix A. Details of model and methods

The electrolyte is modeled in the implicit solvent framework, namely, the interaction potential between two hard-sphere ions is defined by Coulomb's law in a dielectric background when the ions are not overlapped:

$$u_{ij}(r) = \begin{cases} \infty & \text{if} \quad r < d \\ \dfrac{1}{4\pi\epsilon_0\epsilon}\dfrac{z_i z_j e^2}{r} & \text{if} \quad r \geq d \end{cases} \tag{A.1}$$

where r is the distance between two ions. Here, we consider only 1:1 electrolytes, namely, $z_+ = 1$ and $z_- = -1$. The ionic diameters are assumed to be equal for cations and anions: $d = d_+ = d_- = 0.3$ nm. A uniform negative surface charge density σ is placed on the wall of the nanopore.

The z dimension is the one perpendicular to the membrane along the pore. Because the system has rotational symmetry about the z-axis,

the other relevant coordinate is the radial one, r, which represents the distance from the z-axis. The Nernst-Planck (NP) transport equation [32, 33] is used to describe the flow of ions through the pore:

$$\mathbf{j}_i(\mathbf{r}) = -\frac{1}{kT} D_i(\mathbf{r}) c_i(\mathbf{r}) \nabla \mu_i(\mathbf{r}), \qquad \text{(A.2)}$$

where $\mathbf{j}_i(\mathbf{r})$, $D_i(\mathbf{r})$, $c_i(\mathbf{r})$, and $\mu_i(\mathbf{r})$ are the flux density, the diffusion coefficient profile, the concentration profile, and the electrochemical potential profile of ionic species i, respectively. To make use of this equation, we need a relation between the concentration profile, $c_i(\mathbf{r})$, and the electrochemical potential profile, $\mu_i(\mathbf{r})$. Note that we ignore the motion of the solvent here due to the relatively small pore radii and voltages. The electrical and particle current is obtained as

$$I_i = z_i e J_i = z_i e \int_A j_i(\mathbf{r}) \mathrm{d}a, \qquad \text{(A.3)}$$

where $A = R^2\pi$.

In one method, we relate the concentration profile, $c_i(\mathbf{r})$, to the electrochemical potential profile, $\mu_i(\mathbf{r})$, with the Poisson-Boltzmann (PB) theory. This continuum theory is known as the Poisson-Nernst-Planck (PNP) theory.

The other method is based on a Monte Carlo (MC) technique that is an adaptation of the Grand Canonical Monte Carlo (GCMC) method to a non-equilibrium situation, where $\mu_i(\mathbf{r})$ is not constant system-wide: the system is not in global equilibrium, only in local equilibrium. The method is called the Local Equilibrium Monte Carlo (LEMC) technique, while it is called NP+LEMC when we couple it to the NP equation.

In LEMC, the simulation cell is divided into small (about 0.12 nm width) volume elements in the (z,r) plane. We assume local equilibrium in each volume element by fixing the local chemical potential. In the NP+LEMC method, the chemical potential is changed in an iterative process until the $c_i(\mathbf{r})$ and $\mu_i(\mathbf{r})$ profiles provided by LEMC and substituted into the NP equation produce a flux density, $\mathbf{j}_i(\mathbf{r})$ that satisfies the continuity equation, $\nabla \cdot \mathbf{j}_i(\mathbf{r}) = 0$.

References

[1] E. Mádai, B. Matejczyk, A. Dallos, M. Valiskó, D. Boda, Controlling ion transport through nanopores: modeling transistor behavior, Phys. Chem. Chem. Phys. 20 (2018) 24156–24167.

[2] D. Fertig, B. Matejczyk, M. Valiskó, D. Gillespie, D. Boda, Scaling behavior of bipolar nanopore rectification with multivalent ions, J. Phys. Chem. C 123 (2019) 28985–28996.

[3] D. Fertig, M. Valiskó, D. Boda, Rectification of bipolar nanopores in multivalent electrolytes: effect of charge inversion and strong ionic correlations, Phys. Chem. Chem. Phys. 22 (2020) 19033–19045.

[4] Z. Sarkadi, D. Fertig, Z. Ható, M. Valiskó, D. Boda, From nanotubes to nanoholes: Scaling of selectivity in uniformly charged nanopores through the Dukhin number for 1:1 electrolytes, J. Chem. Phys. 154 (2021) 154704.

[5] Z. Sarkadi, D. Fertig, M. Valiskó, D. Boda, The Dukhin number as a scaling parameter for selectivity in the infinitely long nanopore limit: extension to multivalent electrolytes, J. Mol. Liq. 357 (2022) 119072.

[6] D. Fertig, Z. Sarkadi, Valiskó, D. Boda, Scaling for rectification of bipolar nanopores as a function of a modified Dukhin number: the case of 1:1 electrolytes, Mol. Sim. 48 (2022) 43–56.

[7] M. Z. Bazant, K. Thornton, A. Ajdari, Diffuse-charge dynamics in electrochemical systems, Phys. Rev. E 70 (2004) 021506.

[8] K. T. Chu, M. Z. Bazant, Nonlinear electrochemical relaxation around conductors, Phys. Rev. E 74 (2006) 011501.

[9] A. S. Khair, T. M. Squires, Surprising consequences of ion conservation in electro-osmosis over a surface charge discontinuity, J. Fluid Mech. 615 (2008) 323–334.

[10] S. Das, S. Chakraborty, Effect of conductivity variations within the electric double layer on the streaming potential estimation in narrow fluidic confinements, Langmuir 26 (2010) 11589–11596.

[11] L. Bocquet, E. Charlaix, Nanofluidics, from bulk to interfaces, Chem. Soc. Rev. 39 (2010) 1073–1095.

[12] T. A. Zangle, A. Mani, J. G. Santiago, Theory and experiments of concentration polarization and ion focusing at microchannel and nanochannel interfaces, Chem. Soc. Rev. 39 (2010) 1014.

[13] C. Lee, L. Joly, A. Siria, A.-L. Biance, R. Fulcrand, L. Bocquet, Large apparent electric size of solid-state nanopores due to spatially extended surface conduction, Nano Lett. 12 (2012) 4037–4044.

[14] H.-C. Yeh, M. Wang, C.-C. Chang, R.-J. Yang, Fundamentals and modeling of electrokinetic transport in nanochannels, Israel J. Chem. 54 (2014) 1533–1555.

[15] Y. Ma, J. Guo, L. Jia, Y. Xie, Entrance effects induced rectified ionic transport in a nanopore/channel, ACS Sensors 3 (2017) 167–173.

[16] T. Xiong, K. Zhang, Y. Jiang, P. Yu, L. Mao, Ion current rectification: from nanoscale to microscale, Sci. China Chem. 62 (2019) 1346–1359.

[17] A. R. Poggioli, A. Siria, L. Bocquet, Beyond the tradeoff: Dynamic selectivity in ionic transport and current rectification, J. Phys. Chem. B 123 (2019) 1171–1185.

[18] S. D. Cengio, I. Pagonabarraga, Confinement-controlled rectification in a geometric nanofluidic diode, J. Chem. Phys. 151 (2019) 044707.

[19] N. Kavokine, R. R. Netz, L. Bocquet, Fluids at the nanoscale: From continuum to subcontinuum transport, Annu. Rev. Fluid Mech. 53 (2020).

[20] Y. Noh, N. R. Aluru, Ion transport in electrically imperfect nanopores, ACS Nano 14 (2020) 10518–10526.

[21] J. J. Lyklema, A. de Keizer, B. Bijsterbosch, G. Fleer, M. C. S. (Eds.), Solid-Liquid Interfaces, Fundamentals of Interface and Colloid Science 2, Elsevier, Academic Press, 1995.

[22] J. J. Bikerman, Electrokinetic equations and surface conductance. a survey of the diffuse double layer theory of colloidal solutions, Trans. Farad. Soc. 35 (1940)

154.
[23] P. Wiersema, A. Loeb, J. Overbeek, Calculation of the electrophoretic mobility of a spherical colloid particle, J. Coll. Interf. Sci. 22 (1966) 78–99.
[24] R. W. O'Brien, L. R. White, Electrophoretic mobility of a spherical colloidal particle, J. Chem. Soc., Faraday Trans. 2 74 (1978) 1607–1626.
[25] R. W. O'Brien, R. J. Hunter, The electrophoretic mobility of large colloidal particles, Canadian Journal of Chemistry 59 (1981) 1878–1887.
[26] S. Dukhin, Non-equilibrium electric surface phenomena, Adv. Coll. Interf. Sci. 44 (1993) 1–134.
[27] J. Lyklema, M. Minor, On surface conduction and its role in electrokinetics, Colloids and Surfaces A: Physicochemical and Engineering Aspects 140 (1998) 33–41.
[28] J. P. Valleau, L. K. Cohen, Primitive model electrolytes 1. Grand canonical Monte-Carlo computations, J. Chem. Phys. 72 (1980) 5935–5941.
[29] J.-F. Pietschmann, M.-T. Wolfram, M. Burger, C. Trautmann, G. Nguyen, M. Pevarnik, V. Bayer, Z. Siwy, Rectification properties of conically shaped nanopores: consequences of miniaturization, Phys. Chem. Chem. Phys. 15 (2013) 16917–16926.
[30] B. Matejczyk, M. Valiskó, M.-T. Wolfram, J.-F. Pietschmann, D. Boda, Multiscale modeling of a rectifying bipolar nanopore: Comparing Poisson-Nernst-Planck to Monte Carlo, J. Chem. Phys. 146 (2017) 124125.
[31] D. Boda, D. Gillespie, Steady state electrodiffusion from the Nernst-Planck equation coupled to Local Equilibrium Monte Carlo simulations, J. Chem. Theor. Comput. 8 (2012) 824–829.
[32] W. Nernst, Zur kinetik der in lösung befindlichen körper, Zeitschrift für Physikalische Chemie 2U (1888) 613–637.
[33] M. Planck, Ueber die erregung von electricität und wärme in electrolyten, Annalen der Physik und Chemie 275 (1890) 161–186.